Influence of Non-Uniform Aerosol Vertical Density Distributions on Exoplanet Transmission Spectra

A thesis submitted for the degree of

Bachelor of Science

in

Astrophysics

by

Gabriela Michelle Hernandez

Mentors: Mark R. Swain and Gael M. Roudier

Advisor: Jonathan J. Fortney

Thesis Coordinator: David M. Smith

June 1, 2018

Abstract

The study of exoplanets has boomed in efforts to find signs of life, relying on transmission spectra to characterize their atmospheric properties. In this preliminary study, I analyze the influence of uniform and non-uniform aerosol vertical density distributions on exoplanet transmission spectra, focusing on the hot-Jupiter WASP-12b as a prototype for the field. As part of this project, I first disentangled the instrumental parameters of the Hubble Space Telescope (HST) Wide Field Camera 3 (WFC3) from the astrophysical signals to retrieve the transit depth spectrum before validating Cerberus, a radiative transfer and retrieval code used in this study. Using Cerberus and both uniform and non-uniform aerosol distributions to model WASP-12b spectra against actual data, we found that both spectra representing very different atmospheres are both good matches to the actual data. This may indicate that HST-WFC3 data do not fully constrain the non-uniform aerosol vertical density distribution model. However, a positive correlation was found between aerosol density amplitude and gas abundance, thus we expect better constraints on the aerosol model taking into account a non-uniform gas volume mixing ratio (VMR) profile. When uniform and non-uniform aerosol distribution models were projected on the JWST wavelength grid, the models appeared fairly similar for wavelength ranges apart from 2.7-3.1 μm. To draw conclusions about JWST, cases with a non-uniform VMR and a non-uniform aerosol model such as the one produced from this study must be investigated.

Acknowledgements

I would like to thank my research mentors Mark R. Swain and Gael M. Roudier, Yan Betremieux, and Aisha Aiyer for their excellent guidance during the project, the National Aeronautics and Space Administration (NASA) Office of Education for awarding me the Minority University Research Education Project (MUREP) Fellowship through which I was able to contribute to the project, the Jet Propulsion Laboratory (JPL) Office of Education, our project's principal collaborator Robert A. West, and my thesis coordinator David M. Smith and thesis advisor Jonathan J. Fortney for their suggestions and advice. I'd also like to thank my mother Maria Elena Alvarez, my brother Maximiliano Hernandez III, and Giovanni Moreno for their endless support.

Contents

List of Tables

List of Figures

Chapter 1

Introduction

In our quest to characterize exoplanets for signs of life (Sagan et al. 1997), the study of exoplanets and their compositions through transit spectroscopy was first proposed in 2000 by Seager and Sasselov (Seager et al. 2000). We rely on transit analysis via transmission, emission, and phase curve observations to characterize exoplanets. However, only a handful of hot-Jupiter exoplanets can be characterized through all three types of transit observations, making these targets 'prototypes' for the whole field (Fortney et al. 2016). Most of these planets have been found to contain aerosols that have significant consequences on their observed spectra (Sagan et al. 1997, Pavlov el al. 2000, Sing et al. 2014, Zhang et al. 2015, Fortney et al. 2016). As a result, it is important to understand aerosol properties to interpret the data (Kreidberg et al. 2014, Knutson et al. 2014, Fortney et al. 2016).

Although current state-of-the-art exoplanet atmospheric retrieval codes do take aerosols into consideration, most of the existing models assume a uniform aerosol density because it allows for faster recoveries. This assumption is no longer sufficient for the analysis of the new generation of datasets (Fortney et al. 2016), such as spectra from the James Webb Space Telescope (JWST) which is scheduled to launch two years from now (Gardner et al. 2006).

In this study, I analyze the influence of a non-uniform aerosol density distribution on transmission spectrum of the hot-Jupiter WASP-12b. WASP-12b was selected as the target of interest, given that it is one of the largest hot-Jupiters (Hebb et al. 2009) with a dominant water and aerosol component (Kreidberg et al. 2015). As part of the project, I first disentangled the Hubble Space Telescope WASP-12b data and astrophysical signatures to recover the planet's transit depth spectrum. Before analyzing the influence of non-uniform aerosols on WASP-12b's transmission spectrum, it is important to understand how transit data are obtained and how aerosols affect out interpretation of these data.

1.1 Transits and Exoplanet Spectroscopy

The passage of an exoplanet in front of its host star is referred to as its "transit." For a small fraction of systems with low-inclination planetary orbits, transit data are obtained by measuring the dimming of the exoplanet's host star as the exoplanet passes in front of the star. This measurement is referred to as the transit depth. The transit depth is esentially the radius of the planet R_p over the radius of the star R_* squared, or $(R_p/R_*)^2$. In most cases, the change in stellar brightness as a planet passes in front is only about one percent at most, therefore measurements must be taken very carefully. We can represent the flux of the star and the exoplanet's transit visually through a "light curve," such as the one shown in Figure 1.1.

Depending on the wavelength at which an exoplanet is observed, its atmosphere may absorb more of less of light from its host star, causing it to appear physically

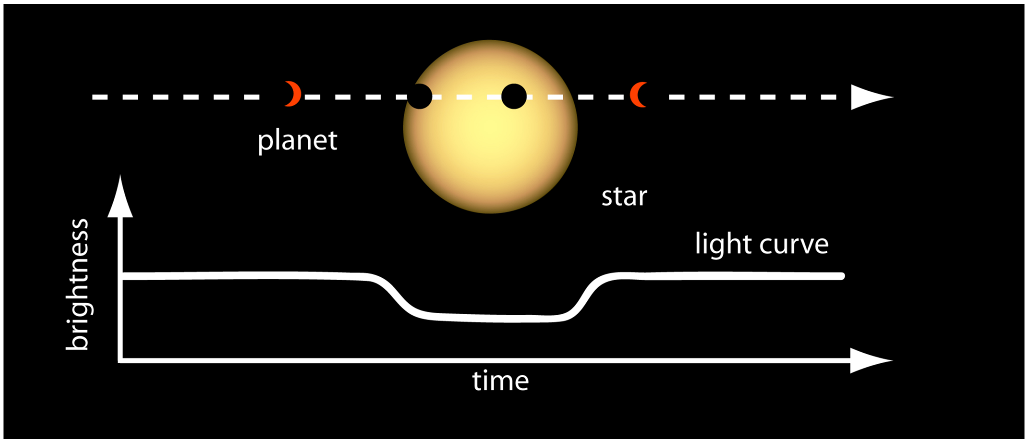

Figure 1.1: The light curve of a star during planetary transit at a certain wavelength. When the planet starts to transit in front of the star, the stellar brightness starts to decrease where the maximum difference between the original stellar brightness and the stellar brightness when the planet is directly in front of the star is the entire light curve by transit depth. The light curve is at its minimum when the planet is near the center of the host star because we assume an extinction law of the surface brightness of the star that depends on the relative positions of the star and planet. Here we can see how the transit depth measured at a certain wavelength, forming a light curve as the stellar flux decreases over time. (NASA 2015).

larger or smaller by a very small amount. If the planet does not have an atmosphere, then the transit depth remains constant at any wavelength, thus reflecting the planets true size for all wavelengths. On the other hand, changes in the transit depth at varying wavelengths indicate the presence of a surrounding atmosphere, where the absorption of photons depends on its composition. In exoplanet spectroscopy, the transmission spectrum formed by the variation of the transit depth as a function of wavelength can then be used to determine the exoplanets atmospheric composition, such as the molecules mentioned in Figure 1.2.

However, aerosols can often impose their own spectral signature on a transmission spectrum. Aerosols are defined as fine solid or liquid particles in the atmosphere that scatter light, such as dust and ice. The scattering of the host star's light can affect an exoplanet's apparent transit depth, subsequently affecting its transmission

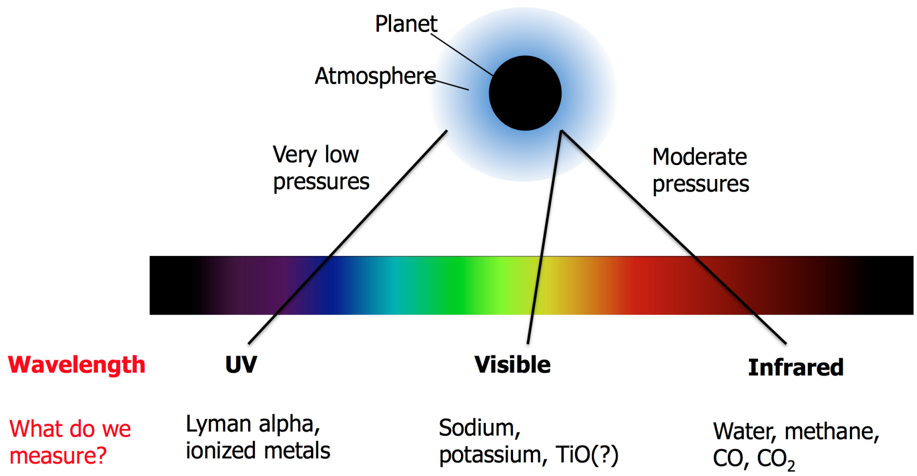

Figure 1.2: These are some of the molecules present in exoplanet atmospheres that are detectable in wavelength range of 100 nm to 50 μm. (Knutson et al. 2012)

spectrum. In cases where an exoplanet's atmosphere is completely saturated by aerosols, the transit depth may change very little if at all, causing an exoplanet's transmission spectrum to appear flat. Futhermore, water absorption lines are seen more prominently in clear exoplanet atmospheres, and are weakest when there are clouds and aerosols involved (Demory at al. 2016). While the opacity slope of exoplanet spectra supports the presence of aerosols in the atmospheres of hot-Jupiters (Swain et al. 2013, Iyer et al. 2015, Zellem et al. 2017), instrument parameters can also have consequences on the interpretation of these data.

As previously mentioned, in this study I analyze the influence of a non-uniform aerosol density distribution on exoplanet transmission spectrum of WASP-12b. To do so, I generated a non-uniform aerosol vertical density distribution model which I implemented into Cerberus, an existing exoplanet radiative transfer and retrieval package created by NASA Jet Propulsion Laboratory exoplanet scientists Gael Roudier and Mark Swain. The data analyzed in this study were collected with the Hubble Space Telescope (HST) Wide Field Camera 3 (WFC3) using the grism 141 filter, which probes absorption features of molecules in the near infrared (IR) wavelength range of 1.1-1.7 μm. As part of the project, I first disentangled Hubble Space Telescope WASP-12b data and instrumental behavior to recover the planet's transit depth spectrum. In the following section, I will provide more details on this process.

Chapter 2

Disentangling HST Instrument Parameters and Astrophysical Signatures for Transit Depth Spectrum Recovery

As previously mentioned, transit light curves exhibit an exoplanet's transit depth modulation as a function of wavelength through which we can constrain its atmospheric composition. The search for H_2O in exoplanet atmospheres has been dominated by transmission measurements obtained with space-based instruments. Although the early detections of H2O in an exoplanet atmosphere were made with the Hubble and Spitzer instruments STIS, IRAC, and NICMOS (Barman 2008; Tinetti et al. 2007; Swain et al. 2008; Grillmair et al. 2008), the leading instrument in this area is the Hubble Space Telescope (HST) Wide Field Camera 3 (WFC3) (Berta et al. 2012; Gibson et al; 2012). In this study, I utilized HST WFC3 data obtained with the G141 IR grism (1.1-1.7 μm) via the Excalibur (EXoplanet CALIbration with Bayesian Unified Retrieval) pipeline.

The Excalibur pipeline gathers public data from a set of different instruments, using Bayesian methodologies to limit the impact of instrumental errors on science parameters. Its strength resides in the growing number of observations for each different target. Excalibur is designed to provide the capability for making the current best estimate in terms of our knowledge of exoplanet atmospheres. For example, changes in a planet's orbital parameters, mass, or improved estimates of the host star temperature, metallicity, or log(g) parameters have the potential to impact science results. To ensure scientific relevance, Excalibur periodically collects new exoplanet data and parameters from multiple archives and incorporates algorithmic, instrument model, and science model updates as they are developed. In other words, the pipeline is event driven, where the events are defined as changes in data or algorithms. When events are detected, dependencies affected by the changes are re-processed. Calibration steps are transparent and quantified using a combination of accessible intermediate state vectors, auto-generation of calibration step documentation, statistical metrics, and Bayesian, evidence-based, model selection capability. Excalibur is designed to provide current, state of the art, calibration and retrieval results to the exoplanet community.

Using HST WFC3 data provided through Excalibur and Markov Chain Monte Carlo (MCMC) methodologies, I performed analysis on correlations between the retrieved instrumental behavior and astrophysical signals. I also quantified the cross-talk between nuisance parameters and the exoplanet transit depth spectrum to ensure that the data I used in my study were cleared of the effects of instrumental parameters.

2.1 Modeling Instrumental Effects on a Light Curve

Before extracting the instrument parameters from real HST data, I modeled the instrumental effects on a theoretical light curve first. HST data was modeled using the Agol model (Mandel Agol 2002), which is a theoretical light curve that describes the dimming of a star when the exoplanet passes in front of it. To keep things simple, I used a linear perturbation as the instrument model, represented by $ax + b$ where a is the slope and b is the intercept. I added both the Agol model and the linear perturbation together to simulate a light curve affected by instrument parameters. This caused the light curve to 'tilt' due to the linear perturbation, as visualized below in Figure 2.1.

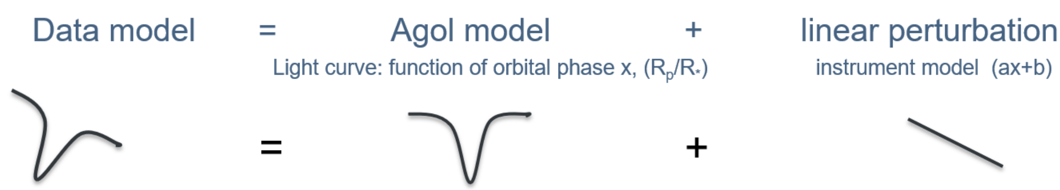

Figure 2.1: Visual representation of the modeled stellar flux, which is a combination of the Agol model that represents theoretical light curve, and the linear perturbation simulates instrumental effects on the light curve.

I then retrieved the parameters of the Agol model and the parameters of the instrument model using a MCMC algorithm which numerically explores the likelihood function by randomly selecting points in the parameter space so that the density of points is higher in the region of interest. Although a more common way of fitting parametrized models to datasets and finding parameters is to minimize the chi-squared, the chi-squared may not yield the main parameters affecting a dataset, especially in more complicated datasets with many parameters. On the other hand, MCMC provides a much better approximation of parameters for more complicated datasets (Gregory 2011), and it includes chi-squared in that the likelihood of a parameter is related to the chi-squared. Using MCMC, we were able to extract probability distributions for the parameters a and b.

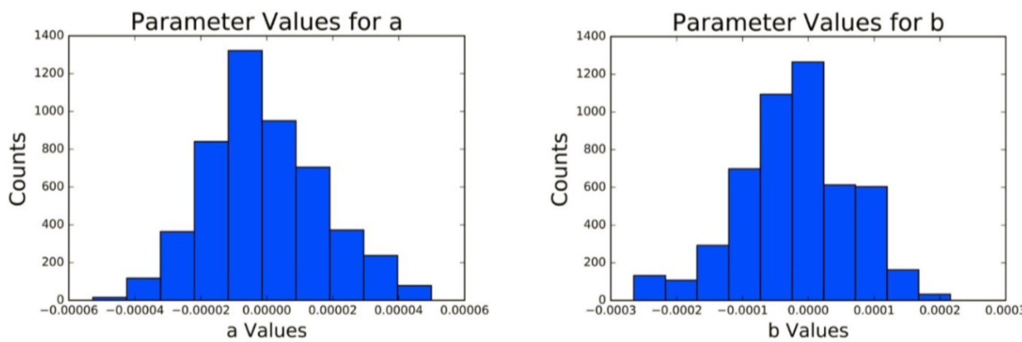

Figure 2.2: Extracted parameters a (slope) and b (intercept) of the linear model.

Using the parameters found, we were able to construct a data model of the white light curve that best fit the actual HST data. A white light curve is the average of all light curves for available wavelengths. Figure 2.3 shows the best fit model against actual HST data. Separation z is the distance between the center of the host star and the center of the planet.

Extracting the most likely set of parameters to construct a white light curve that best fit the actual data was simple due to the fact that we modeled a linear perturbation across a whole visit, but actual data may include linear trends inside each orbit. A visit slope can be observed across a whole light curve, whereas orbit slopes appear across various times in a white light curve across a visit. It is quite evident that there is not only a linear trend across the whole visit, but that there

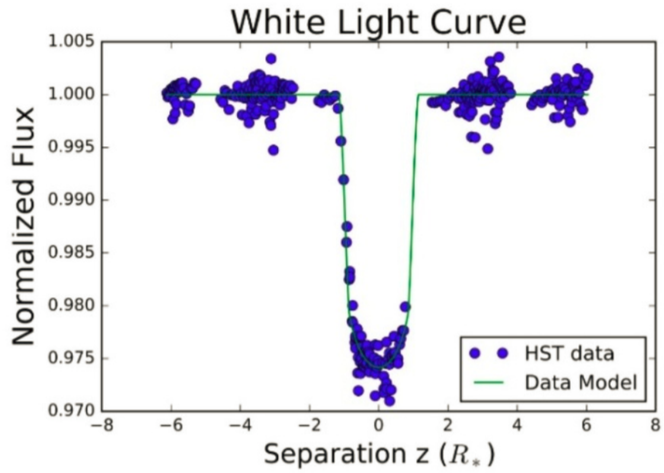

Figure 2.3: Model white light curve generated using simulated instrument parameters a and b (green) against actual HST data (blue).

also appears to be a trend within each orbit, as shown in Figure 2.4.

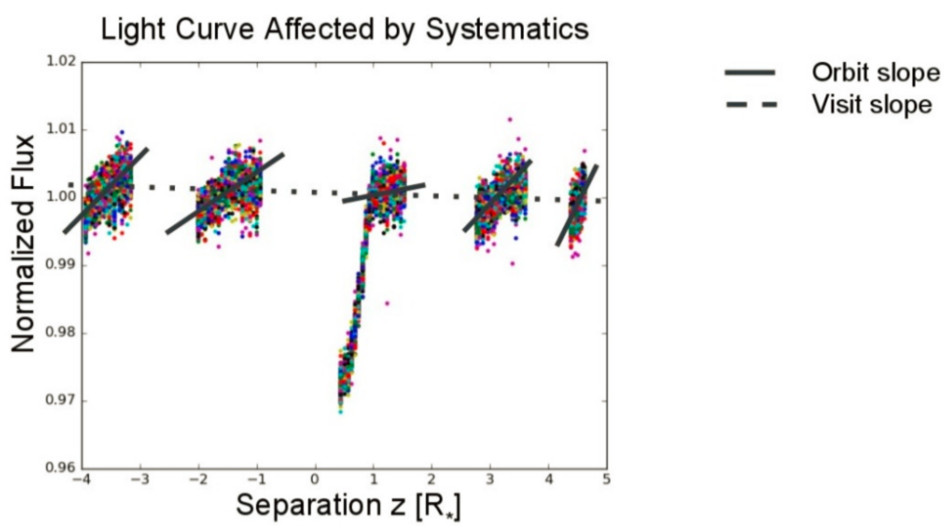

Figure 2.4: More complicated, realistic instrument models feature orbit specific trends in addition to the visit trend.

For more complicated datasets, a more complex instrument model is needed to extract all parameters and then find the parameter sets with the highest correlation to the transit depth in the light curve. The model used in Excalibur products takes orbit specific trends into account in addition to the visit trend in order to find the main instrument parameters that are tampering with the astrophysical signal.

2.2 Extracting Correlations Between Transit Depth Spectra and Parameter Spectra

To rank the main instrument parameters, I computed the Pearson Correlation Coefficient for the transit depth spectrum and the instrument parameter spectrum using the equation $\rho_{X,Y} = \frac{\overline{XY} - \bar{X}\bar{Y}}{\sigma_X \sigma_Y}$ where X is the transit depth spectrum and Y is the instrument parameter spectrum. Both the transit depth spectrum and the instrument parameter spectrum are shown in Figure 2.5.

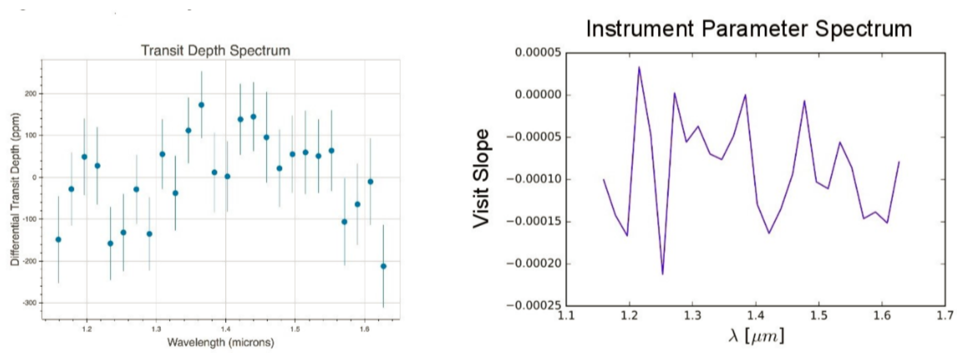

Figure 2.5: To find the main nuisance parameters, the instrument parameters from the right plot with the highest correlations to the transit depth spectrum from the left plot were extracted.

By comparing their Pearson Correlation Coefficients, we can infer the relationship between parameters and spectra. Once I computed the correlations for each of the parameters, I found the Pearson Correlation Significance Threshold, which indicates whether a parameters effect is significant or not. If any of the correlations have an absolute value greater than its respective Pearson Correlation Threshold, this indicates that the correlation is significant between that parameter and the transit depth. The results are summarized in Table 2.1.

	Pearson Correlation Coefficient (%)
Transit Depth and Visit Slope	3.8
Transit Depth and Visit Intercept	-21.0
Transit Depth and Orbit Slope 1	9.0
Transit Depth and Orbit Slope 2	6.7
Transit Depth and Orbit Slope 3	8.3
Pearson Correlation Coefficient Threshold	9.7

Table 2.1: Correlations between the transit depth and various instrument parameters larger in magnitude than the Pearson Correlation Coefficient Threshold may be leaking into the transit depth spectrum.

Since the correlation between the transit depth and the visit intercept was -21.0% which is greater than its threshold value of 9.7%, this indicates that the visit intercept instrument parameter may be leaking into the transit depth spectrum, therefore affecting the interpretation of the exoplanet atmospheres abundances. However, this contamination from the the instrument can be taken into account when extracting the atmosphere abundances. Since we know the signature of the instrument contamination as shown in Figure 2.6, this can be used as a template for the Cerberus radiative transfer model to account for its effects on the retrieved atmosphere abundances.

With these findings, I was able to apply MCMC methodologies to the Excalibur data, yielding the main nuisance instrument parameters for every target in the pipeline. Essentially, the process detailed in this section was repeated for all targets. The first part of the project involving the separation of instrument parameters and data is completed.

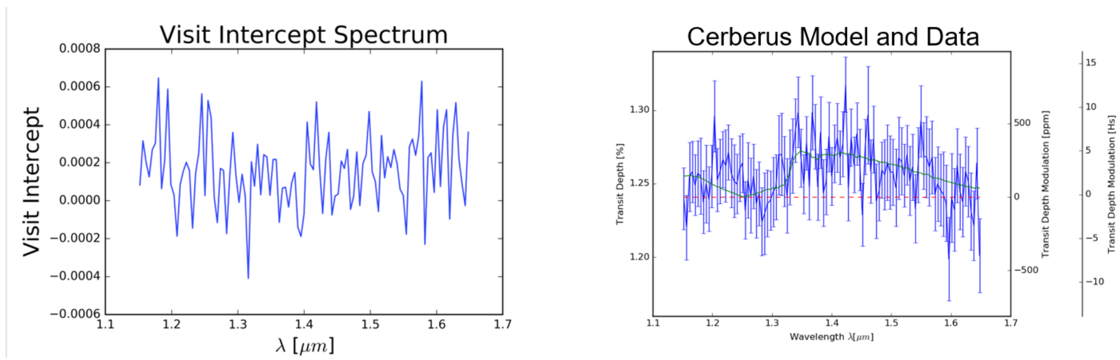

Figure 2.6: The known signature of the visit intercept on the left will be taken into account when modeling transmission spectra, such as shown on the right

Chapter 3

Validating Cerberus Radiative Transfer and Retrieval Model

Once I disentangled the instrumental parameters from the astrophysical signatures for each target in the Excalibur pipeline, my next step before starting analysis on aerosols was to validate Cerberus, the radiative transfer forward model I used in this project. Cerberus runs many spectra to fit a dataset, and yields the model that best fits the data to find relevant atmospheric parameters.

To validate Cerberus, I first created a water-dominated exoplanet atmosphere model. Once the simulation of the water-dominated atmosphere was made, I added random Gaussian noise to the atmosphere with sigma equal to 100 ppm. I then compared the input values listed in Table 3.1 with the simulated exoplanet atmosphere with the output values returned by Cerberus, knowing that if the input values matched the output values fairly well, this would indicate that Cerberus is not biased.

Simulated Exoplanet Atmosphere Input Characteristics
Log(H_2O) [ppm]: .1 (10 ppm)
Temperature: 900 K
Negligible abundances for molecules other than H_2O
No clouds

Table 3.1: Input values for the simulated exoplanet atmosphere.

Once I generated a simulated atmosphere with these quantities, Cerberus returned the water distributions shown in Figure 3.1 at three different resolutions.

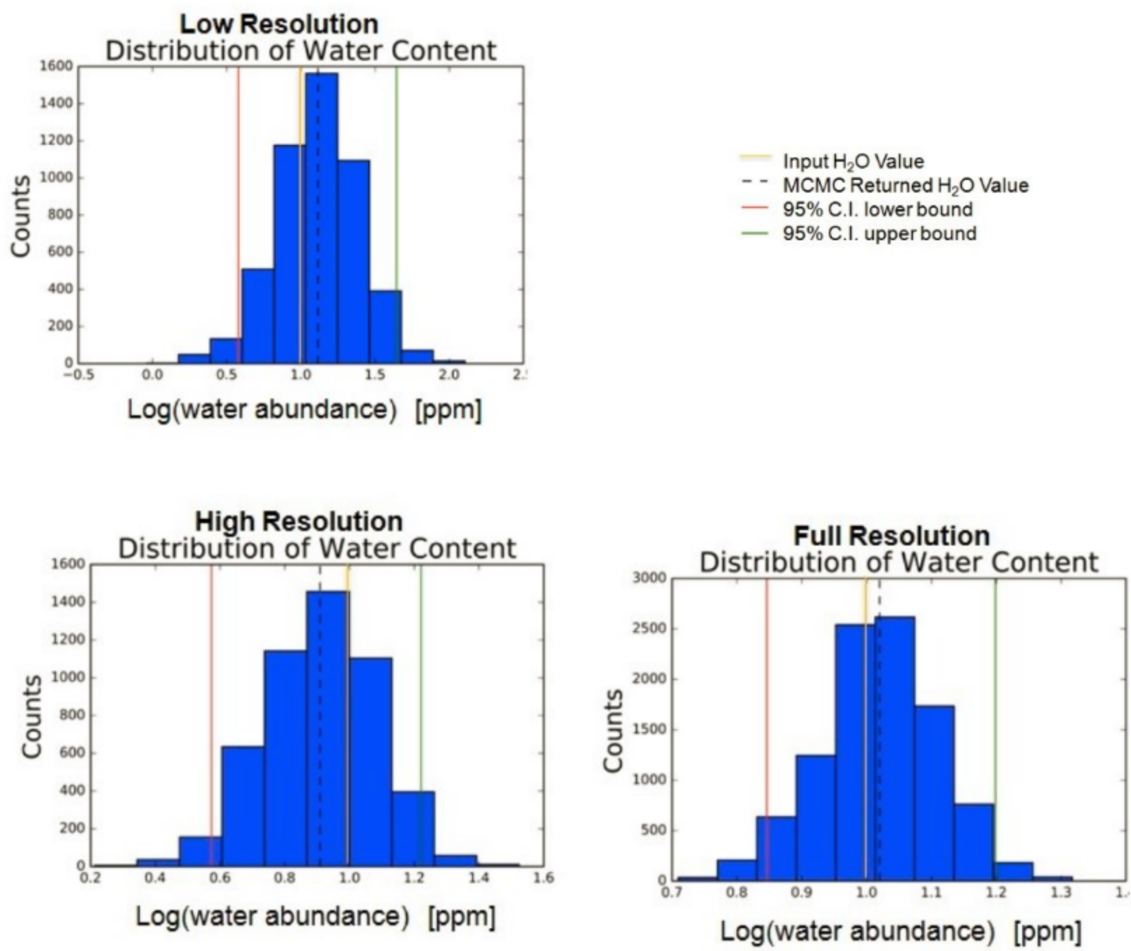

Figure 3.1: Water distributions at low, high, and full resolutions. The output value Ceberus returned for log water abundance are marked by the dashed black lines, and the inputs are represented by solid yellow lines. Two sigma bounds enclosing a 95% confidence interval are represented by the red and green lines.

The output values Ceberus returned are fairly close to the input values, which are within two sigma bounds for all three resolutions. In other words, the water abundance output values are each compatible with the input values within a 95% confidence interval, therefore indicating that the Cerberus retrieval code does not appear to be biased. This finding indicates that Cerberus may be used to reliably retrieve water content in exoplanet atmospheres.

Chapter 4

Influence of Non-Uniform Aerosol Density Distributions on Exoplanet Transmission Spectra

Now that I've disentangled the HST WFC3 exoplanet data from instrumental parameter effects and validated the Cerberus radiative transfer model, I can start analyzing the effects of non-uniform aerosol density distributions on exoplanet transit spectra.

Recall that aerosols can impose their own spectral signature on transmission spectra. For this reason, it is necessary to account for aerosols in exoplanet atmosphere models to interpret an exoplanet's atmosphere (Sing et al. 2015). By analyzing the effects of non-uniform aerosol density distributions on spectra, we can anticipate the needs in forward model accuracy for future datasets and understand the interaction between gas and aerosol cloud parameters. In this project I modified Cerberus with a non-uniform aerosol density distribution model, and retrieved correlations between cloud and atmosphere properties, focusing on the water content in WASP-12b's atmosphere.

4.1 Basic Structure of the Cerberus Model

Since the aerosol density distribution model is just a component of the exoplanet atmosphere model within Cerberus, the model has components from both gases and aerosols. An exoplanet's overall spectral signature is mainly related to the total optical depth τ as shown below, which is dependent on the contributions from both the absorption component of the gas and the scattering component from aerosols in an exoplanet's atmosphere.

$$\tau_{gas} + \tau_{aerosols} \tag{4.1}$$

The optical depth τ due to aerosols is modeled by a simple power law as a function of wavelength λ in the scattering regime as shown below (Mischenko et al. 1997, Sing et al. 2013). Knowing that Rayleigh scattering is among the best fitting models, we assume averaged Rayleigh scattering in our study (Sing et. al. 2013).

$$\tau_{aerosols} = n_z(\frac{\lambda}{\lambda_o})^{-\beta} l_z \tag{4.2}$$

The aerosol contribution is then a combination of the scattering law and the aerosol density as a function of altitude z. In the equation above, n_z represents the aerosol vertical density profile at altitude z, β is the scattering index, l_z is the optical path length at altitude z, λ is the wavelength, and λ_o is the normalization factor dependent on the physical nature of the aerosol. In this study, I construct the aerosol vertical density distribution n_z.and implement this into the existing Cerberus atmospherc retrieval model.

4.2 Parametrizing and Constructing The the Non-Uniform Aerosol Density Distribution

To parametrize the non-uniform aerosol model n_z, I utilized Jupiter vertical non-uniform aerosol density distribution data as a basis for the exoplanet aerosol model. The data used for the parametrization is the number density data of Jupiter's stratosphere and upper troposphere above 0.2 bar, retrieved by near-infrared (NIR) range ground-based observations combined with Cassini/International Space Station (ISS) images (Ulyana et al. 2013). We note that the number density of hazes are closely related to the optical properties of the particles.

At different latitudes on Jupiter, the vertical aerosol density distributions differ. This means that for each pressure level, the aerosol number density differs when it is measured at different latitudes. After analyzing Jupiter's vertical density profiles at different latitudes, I retrieved the median aerosol vertical density distribution shown in Figure 4.1 by taking the median number density at each pressure level. This median aerosol vertical density profile was used as a basis for the parametrization.

Since Jupiter's vertical density profiles and median aerosol vertical density profile reflect Gaussian distributions in log pressure, I opted to use a Gaussian parametrization for the aerosol model n_z.

$$n_z = Ae^{-\frac{1}{2}(\frac{logP - logP_a}{\sigma})^2} \tag{4.3}$$

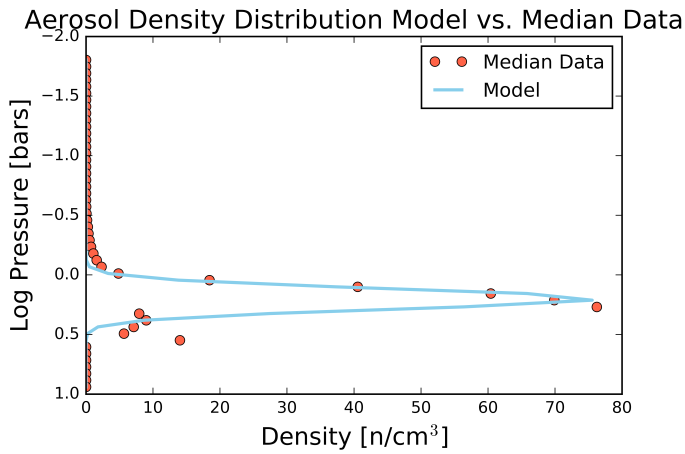

Figure 4.1: Median aerosol vertical density distribution data is represented by the orange points against the aerosol vertical density distribution model shown by the blue curve. The y-axis scaling represents a log or a power of ten, where 1 in log pressure [bars] represents a pressure of ten bars in Jupiter's atmosphere.

In the aerosol model, P is the atmospheric pressure, and the free parameters P_a, A, and σ are aerosol cloud pressure level, aerosol density amplitude, and aerosol cloud thickness respectively.

4.3 Testing the Non-Uniform Aerosol Model on Jupiter Data

Once the aerosol model was parametrized, the model was tested on Jupiter's median aerosol density distribution to verify that the model is at least valid for solar system planets. A plot of the model fitting the data is shown in Figure 4.1.

The retrieved parameters for the fit of the model to Jupiter's median aerosol density profile were P_a=1.6 bars, A=76 cm^{-3}, and σ=0.1. We use this approximate value of the aerosol density amplitude A in the Cerberus aerosol model as a reference value for exoplanets. In other words, the retrieved amplitude for exoplanets is a multiplication factor of Jupiter's retrieved value for A. Sigma can be interpreted as the vertical spread of the aerosol cloud, where σ is the exponent to a base of ten. This number is the multiplication factor of the average pressure. For example, if σ=1, this means that the lower limit of the cloud is at a pressure ten times higher than the average pressure, and the higher limit is at a pressure level 10 times lower than the average pressure. The average pressure, or the location where the cloud is centered, is P_a.

4.4 Generating Exoplanet Forward Models with Varying Quantities of Aerosols

After creating the aerosol model, the next step was to explore how the transmission spectra generated by Cerberus changed as a result of the model by varying various parameters. After creating the aerosol vertical density distributions shown in Figure 4.2 using the aerosol model newly implemented into Cerberus, the spectra shown in Figure 4.3 were retrieved for a typical hot-Jupiter. Using the magenta, non-uniform aerosol distribution and the green, almost uniform distributions, I generated forward models of transmission spectra in their respective colors.

As expected, the spectral signature of water becomes flatter as the aerosol cloud becomes denser. In other words, water is easier to detect in clear atmospheres, whereas its features appear weakest in a clouded atmosphere (Demory et al. 2016). It is important to note that these are not physical cases since the spectra shown in Figure 4.3 were only generated with the premise of exploring the impact of the parametrization of the aerosol model on the spectra. Given that the aerosol model

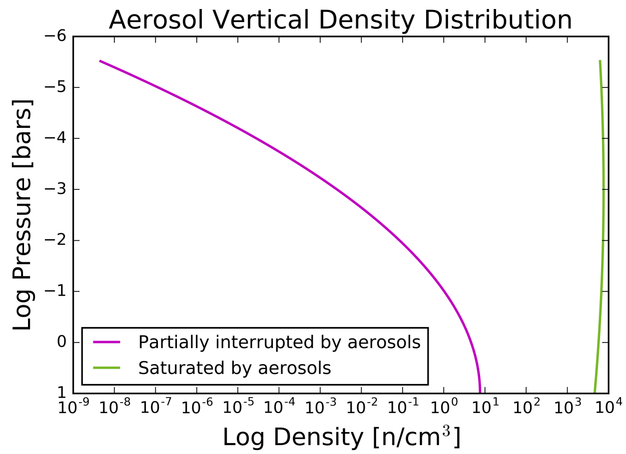

Figure 4.2: A non-uniform aerosol vertical density distribution profile in magenta, which partially interrupts transmission spectra. The green aerosol distribution is denser and uniform, which would completely saturate an exoplanet's atmosphere.

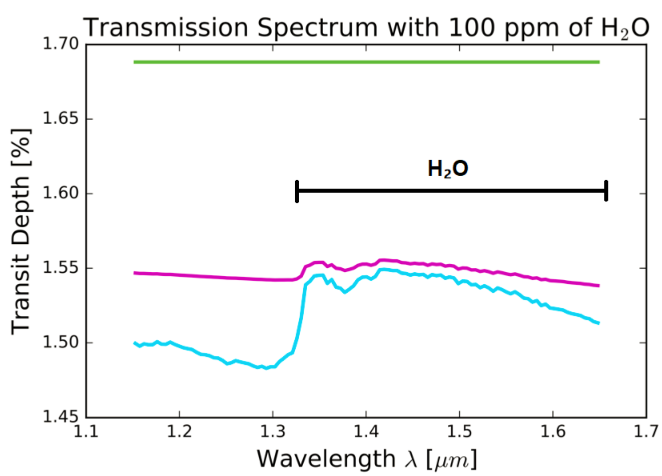

Figure 4.3: The blue spectrum represents a hot-Jupiter with a clear atmosphere and 100 ppm of water. The magenta spectrum is partially impacted by aerosols, containing 100 ppm of water and one-tenth the amount of Jupiter's aerosol median number density (76 cm^{-3}), with the aerosol cloud centered at ten bar. The green spectrum is completely saturated by aerosols, containing 100 times Jupiter's aerosol density, with the cloud centered at one mbar and a huge spread that covers the entire atmosphere, thus causing the spectrum to appear flat.

impacted the spectral modulations shown in the previous figure, the next step was to use real exoplanet data to constrain the parameters of the aerosol model and to see what kinds of values/errors would be obtained from data.

4.5 WASP-12b Transmission Spectrum Recovery Utilizing the Non-Uniform Aerosol Model

For the exoplanet spectrum recovery, I used data from the Hubble Space Telescope (HST) provided by the Excalibur Pipeline for the target WASP-12b. This target was the focus of my study, since it is believed to have a dominant water signature and an aerosol component in its spectrum (Kreidberg et al. 2015). To compare the effects of non-uniform and uniform aerosol density distributions on exoplanet spectra, I used both distributions to recover the transmission spectrum for WASP-12b. For the non-uniform aerosol density distribution, I varied the water abundance, aerosol density amplitude, aerosol pressure level, and scattering index. For the uniform aerosol density distribution, I varied only the water abundance and the aerosol density amplitude. The parameters shown in Table 4.1 for these variables were retrieved using the Markov Chain Monte Carlo (MCMC).

Retrieved Parameters	Non-Uniform Dist.	Uniform Dist.
Water abundance	1000 ppm	100 ppm
Aerosol density amplitude	152 cm^{-3}	380 cm^{-3}
Aerosol pressure level	9 bars	
Aerosol cloud thickness	1.0	

Table 4.1: The free/retrieved parameters used to generate the aerosol vertical density distributions shown in Figure 4.4.

Note that for the non-uniform distribution, the aerosol density amplitude is about twice as much as Jupiter's, and the uniform distribution has an aerosol density amplitude five times as much as Jupiter's. Using the retrieved parameters from Table

4.1, I then generated non-uniform and uniform aerosol density distributions shown in Figure 4.4. Once the the non-uniform and uniform aerosol models were generated, I incorporated both into Cerberus, which yielded the transmission spectra shown in Figure 4.5.

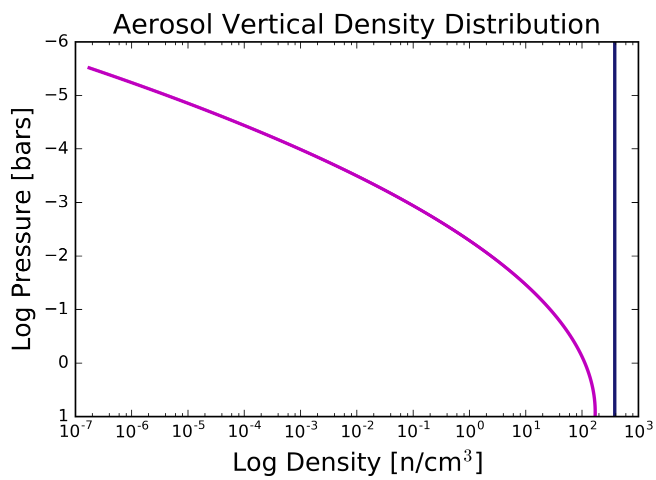

Figure 4.4: The uniform aerosol distribution in blue features a number amplitude A five times Jupiter's aerosol density, and its atmosphere contains about 100 ppm of water. The non-uniform distribution in magenta contains a water abundance of about 1000 ppm, with a cloud centered at 9 bars and an aerosol density amplitude twice as much as Jupiter's aerosol density.

The spectra look similar despite the fact that the non-uniform distribution features a higher aerosol density amplitude and predicts less aerosols than the uniform distribution. The difference between the spectral modulations is less than one sigma, or the typical error bar of a data point. From Figure 4.5, we can observe that neither of the models compensate for outlying data points or the peak feature found at approximately 1.19 microns, which may be due to an aerosol signature, a missing gas absorber, or system residuals. Note that some deviations between the data and each model appear to be larger than the deviation due to these two different models. The water abundance between the two spectral modulations differs by one order of magnitude. Since one order of magnitude is the size of the error bars we typically

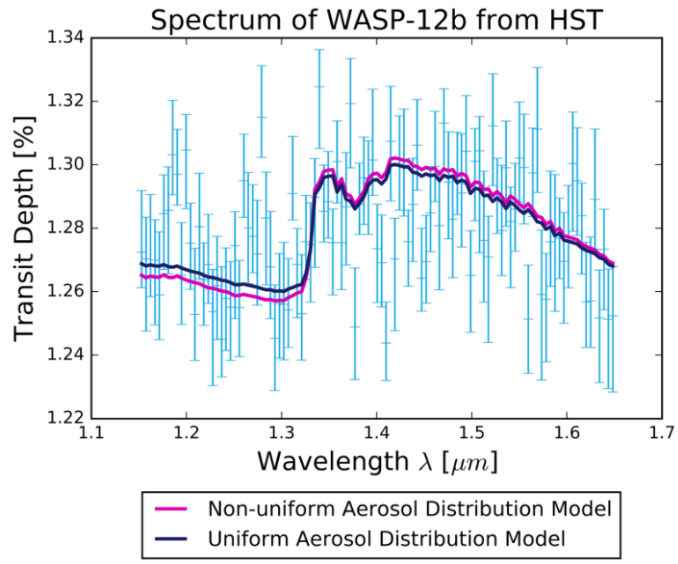

Figure 4.5: Two transmission spectra shown against the data in light blue. The spectra for the target WASP-12b were produced using the uniform and non-uniform distributions shown in Figure 4.4. The non-uniform aerosol vertical density distribution in magenta was used within Cerberus to create the magenta non-uniform transmission spectrum, whereas the uniform distribution shown in navy yielded the navy transmission spectrum shown on this plot.

expect with current radiative transfer codes, the two spectral modulations both fit the data closely if outliers are neglected. In other words, very different atmospheres (one with uniform aerosol clouds and another with non-uniform aerosol clouds) yield similar spectra that are both good matches to the actual data overall, but neither model compensates for outliers. In addition, the resulting fits indicate that the non-uniform and uniform aerosol models converge on a removed spectrum that's extremely similar in the HST wavelength band.

Depending on aerosol level or the wavelength at which a target is observed, one may be able to probe higher or deeper into an exoplanet's atmosphere. Since HST is confined to probe between 1 bar and 1 mbar, HST data has limitations. The results indicate that HST/G141 does not fully constrain the non-uniform model, but this tool will important when dealing with much higher signal-to-noise JWST data.

4.6 Correlations between Non-Uniform Aerosol Model Parameters

To investigate the correlations between the non-uniform aerosol model parameters, we visualize their interactions as well as the interaction between the parameters and the gas abundances as shown in Figures 4.6-4.8. In the correlation plots, each point is a "visit" of the MCMC.

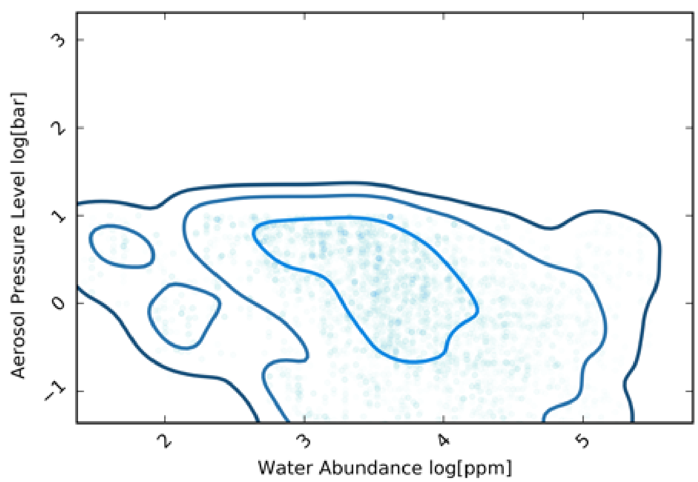

Figure 4.6: There is a negative correlation between the water abundance and the aerosol cloud pressure level, or the location of the aerosol cloud.

From the retrieved correlations, we see that there is crosstalk between all the parameters. Since the constraints are not very good, it's difficult to interpret the correlations. One limitation of the newly created non-uniform aerosol model is that it isn't realistic to allow the cloud model of a finite thickness to be at any arbitrary

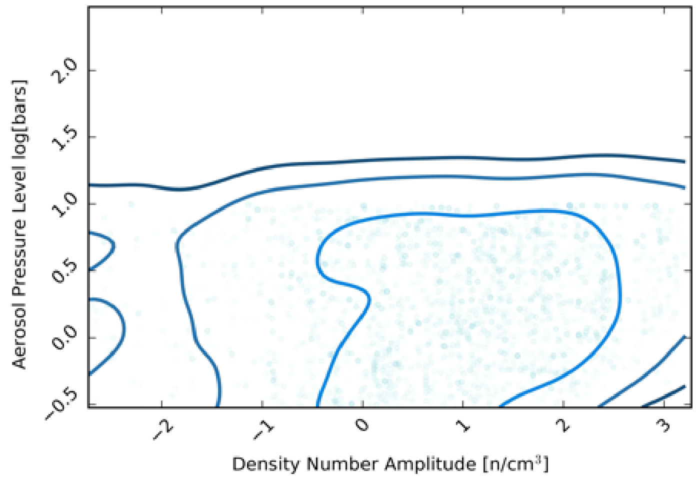

Figure 4.7: The correlation plot above shows a weak correlation (if any) between the density number amplitude and the aerosol cloud pressure level.

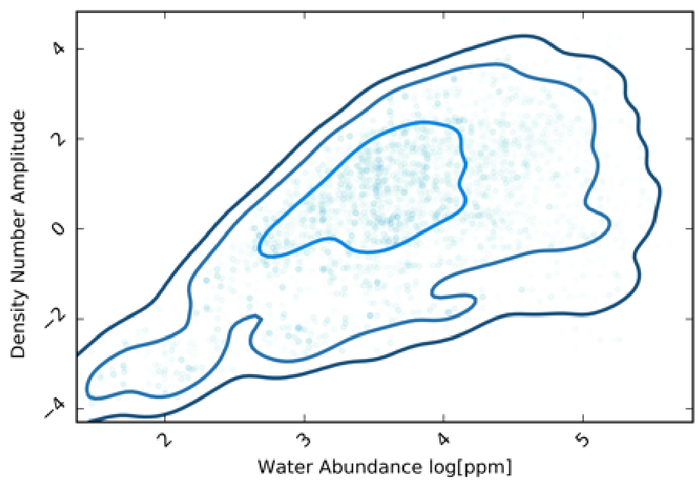

Figure 4.8: There is a very strong positive correlation between the water abundance and the density number amplitude, as there is a visible upward slope.

altitude, since a dense clouds can hardly be sustained high in the atmosphere.

4.7 JWST Forecast

With JWST scheduled to launch within the next two years, we can anticipate a new influx of knowledge regarding our understanding of planets. The telescope will be stationed nearly a million miles from Earth, using a 21.3-foot (6.5-meter) mirror and four science instruments (Clark, Stephen) to observe transiting planets, revealing the their atmospheric compositions, structures, and dynamics. (Bean, et al.) To prepare for the analysis of JWST data, I generated some forecasts. The two models (uniform and non-uniform) were projected on the JWST wavelength grid as shown in Figure 4.9. The uniform model was used to simulate JWST data, and these were then compared to the uniform model to see if they would agree or differ significantly.

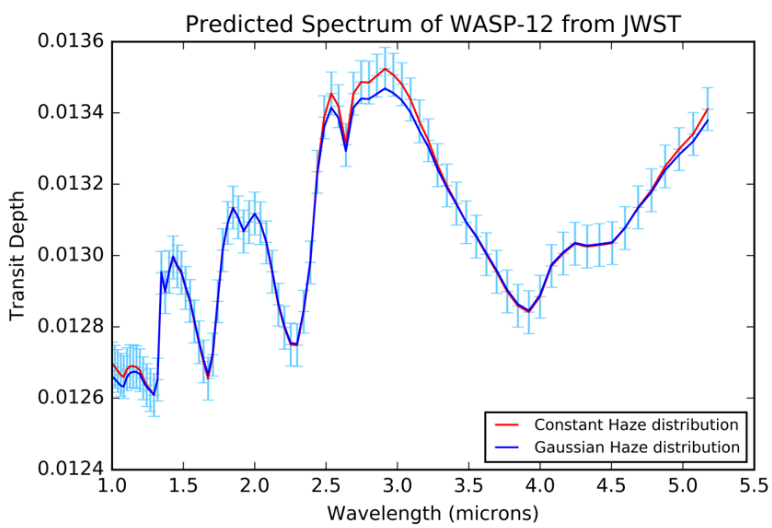

Figure 4.9: The predicted spectra for the target WASP-12b from JWST data in orange contains a uniform aerosol distribution, and the predicted spectrum in royal blue was generated using the Gaussian, non-uniform aerosol distribution. Both models are shown against the simulated JWST data in light blue, which is based on a uniform hypothesis. The data points are evenly spaced in frequency rather than wavelength. The error bars are standard error bars in python.

The models appear fairly similar, except in the middle region which probes a wavelength range between 2.7-3.1 microns. Figure 4.10 shows a closer view of the predicted spectra within this wavelength range.

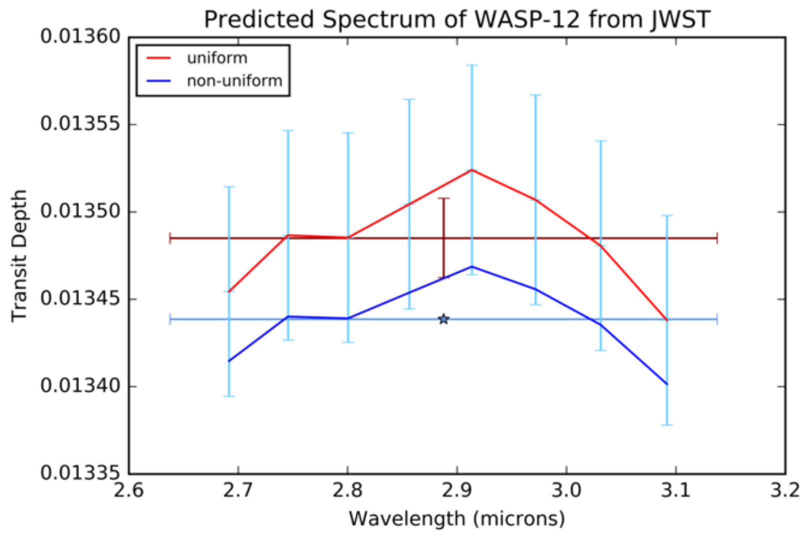

Figure 4.10: A closer view of the predicted spectra for the target WASP-12b for JWST within the wavelength range from 2.7-3.1 microns. The simulated data in light blue was generated under a uniform hypothesis. The spectrum in orange contains a constant or uniform aerosol distribution, whereas the predicted spectrum in royal blue was generated using a Gaussian, non-uniform aerosol distribution. The rust colored bar represents the average of the eight data points and the error on the average, while the pale blue colored bar is the average of the non-uniform predicted spectrum. The average of the non-uniform, blue model over that same range is indicated by the star.

The data between 2.7-3.1 microns were averaged in one bin, and the non-uniform model was also averaged. The distance between the average of the uniform model in one representative JWST bin and average of the the non-uniform model in the same bin being considered was found to be 1.907 sigma. This error was appropriated by dividing the forecasted JWST error bar for one data sample by the square root of the number of samples in this JWST bin. Since this value is about two sigma, this statistically starts to be significant. However, there's not a strong distinction between the two models when systematics are taken into account. This result implies that JWST might be able to probe this region in favorable cases. Depending on the aerosol cloud levels or the wavelength at which targets are observed, we are able to probe deeper into an exoplanet's atmosphere. From this study, we can observe that the HST data do not fully constrain the non-uniform aerosol vertical density distribution model, and that there is a lot of crosstalk between all aerosol model parameters. In particular, there is a positive correlation between the aerosol density amplitude and the gas abundance. To gain a better understanding, further work must be done to derive how significant the difference between the two models is within this region by taking into a account a non-uniform volume mixing ratio and more rigorous aerosol modeling, spherical shells, and a full Mie scattering code to compute the effective optical depth of aerosols as a function of wavelength.

Chapter 5

Conclusion

From this study, two very different atmospheres (one with uniform aerosol clouds and another with non-uniform aerosol clouds) yield similar spectra that are both overall good matches to the actual data when neglecting outliers. We see that the HST data do not fully constrain the non-uniform aerosol vertical density distribution model, but this tool will be significant when dealing with much higher signal-to-noise JWST data. We expect better constraints on the aerosol model by taking into account the distribution of the gas abundance as a function of altitude, spherical shells, and Mie scattering. In addition, it is evident that there is a lot of crosstalk between all the aerosol model parameters, and we were able to see a positive correlation between aerosol density amplitude and gas abundance in exoplanet atmospheres. Since there is a correlation between aerosol density amplitude and gas abundance, we expect better constraints on the aerosol model taking into account the distribution of the gas abundance as a function of altitude. This depends strongly on volume mixing ratio profile.

This is a preliminary study assuming that the gas in the atmosphere is uniformly mixed, since there is a correlation between the water abundance and the quantity of aerosols, which are the two main components in the shape of the spectrum. To draw conclusions about JWST, we must analyze a case with a non-uniform mixing ratio, Mie scattering, and the non-uniform aerosol model produced from this study.

Bibliography

NASA. Light Curve of a Planet Transiting Its Star. NASA, National Aeronautics and Space Administration, 16 Apr. 2015.

Barman, T. 2007 Identification of Absorption Features in an Extrasolar Planet Atmosphere. *Astrophys. J.*, 661, L191L194.

Bean, J. L. et al. 2018 The Transiting Exoplanet Community Early Release Science Program for JWST. *Astrophys. J.*.

Berta, Z. K. et al. 2012 The Flat Transmission Spectra of the Super-Earth GJ1214b from Wide Field Camera 3 on the Hubble Space Telescope. *Astrophys. J.*, 747, 35.

Clark, Stephen. Webb Telescope's Launch Delayed until 2020. Spaceflight Now — Falcon Launch Report — Successful Launch for Falcon 1 Rocket, Spaceflight Now/ Pole Star Publications Ltd, 27 Mar. 2018, spaceflightnow.com/2018/03/27/webb-telescopes-launch-delayed-until-2020/.

Demory, Brice-Oliver, et. al. 2016. A continuum from clear to cloudy hot-Jupiter exoplanets without primordial water depletion. *The Astrophysical Journal Letters.*

Fortney, J. J., et al. 2016 The Need for Laboratory Work to Aid in The Understanding of Exoplanetary Atmospheres. *Astrophys. J.*

Gardner J. P., et al. 2006 The James Webb Space Telescope. *Space Science Reviews*, 485-606.

Gibson, N. P., et al. 2012 Probing the haze in the atmosphere of HD 189733b with HST/WFC3 transmission spectroscopy. MNRAS, 422, 753.

Gregory, P. C., Bayesian exoplanet tests of a new method for MCMC sampling in highly correlated model parameter spaces, Monthly Notices of the Royal Astronomical Society, Volume 410, Issue 1, 1 January 2011, Pages 94110.

Grillmair, C. J., et al. 2008 Strong water absorption in the dayside emission spectrum of the planet HD189733b. *Nature*, 456, 767769.

Hebb L. et al. 2009 WASP-12b: The Hottest Transiting Extrasolar Planet Yet Discovered. *Astrophys. J.*, 693, 1920.

Iyer, A.R., et. al. 2015 A Characteristic Transmission Spectrum Dominated by H_2O Applies to the Majority of HST/WFC3 Exoplanet Observations. *Astrophys. J.*

Knutson, Heather, 2012. Introduction to Transit (and Secondary Eclipse) Spectroscopy.

Knutson, H. A., et al. 2014 A featureless transmission spectrum for the Neptune-mass exoplanet GJ436b. *Nature*, 505, 66-68.

Kreidberg, L., et al. 2014 Clouds in the atmosphere of the super-Earth exoplanet GJ1214b. *Nature*, 505, 69-72.

Kreidberg, L., et. al. 2015 A Detection of Water in the Transmission Spetrum of the Hot Jupiter WASP-12b and Implications for its Atmospheric Composition. *Astrophys. J.*.

Mandel, K., Agol, E. 2002 Analytic Light Curves for Planetary Transit Searches. *Astrophys. J.*, 580:L171L175.

Mishchenko, M. I., et al. 1997. Modeling Phase functions for dustlike tropospheric aerosols using a shape mixture of randomly oriented polydisperse spheroids. *Journal of Geophysical Research*.

Pavlov A. A., et al. 2000 Greenhouse warming by CH4 in the atmosphere of early Earth, *Journal of Geophysical Research*, 105 (2000): 11981-11990.

Sagan C., Chyba C. 1997 The early faint sun paradox: Organic shielding of ultraviolet-labile greenhouse gases. *Science*, 276, 1217-1221.

Seager, S., Sasselov, D. D. 2000 Theoretical Transmission Spectra during Extrasolar Giant Planet Transits. *Astrophys. J.*, 537, 916921.

Swain, M. R., et al. 2013 Probing the extreme planetary atmosphere of WASP-12b. *Elsevier*.

Swain, M. R., et al. 2008 The presence of methane in the atmosphere of an extrasolar planet. Nature, 452, 329331.

Sing, D. K., et al. 2013, HST hot Jupiter transmission spectral survey: evidence for aerosols and lack of TiO in the atmosphere of WASP-12b. MNRAS, 436, 2956

Sing, D. K., et al. 2015 HST hot-Jupiter transmission spectral survey: detection of potassium in WASP-31b along with a cloud deck and Rayleigh scattering. MNRAS, 446, 2428

Tinetti, G., et al. 2007 Infrared Transmission Spectra for Extrasolar Giant Planets. *Astrophys. J.*, 654, L99L102.

Zellem, R. T., et. al. 2015 Forecasting the Impact of Stellar Activity on Transiting Exoplanet Spectra. *Astrophys. J.*.

Zhang, X., et al. 2013 Stratospheric Aerosols on Jupiter from Cassini Observations. Icarus 226, 1, 159-171

Zhang, X., et al. 2015 Aerosol Influence on Energy Balance of the Middle Atmosphere of Jupiter. *Nature*, 10231. PMC. Web. 24 May 2018.